Journal of Foraminiferal Research, v. 50, no. 2, p. 204–218, April 2020

TRACE ELEMENT HETEROGENEITY ACROSS INDIVIDUAL PLANKTIC FORAMINIFERA FROM THE MODERN CARIACO BASIN

Catherine V. Davis[1,2,*], Jennifer S. Fehrenbacher[3], Claudia Benitez-Nelson[1] and Robert C. Thunell[1,†]

ABSTRACT

The trace element composition of planktic foraminifera shells is influenced by both environmental and biological factors ('vital effects'). As trace elements in individual foraminifera shells are increasingly used as paleoceanographic tools, understanding how trace element ratios vary between individuals, among species, and in response to high frequency environmental variability is of critical importance. Here, we present a three-year plankton tow record (2010–2012) of individual shell trace element (Mg, Sr, Ba, and Mn) to Ca ratios in the planktic species *Globigerina ruber* (pink), *Orbulina universa*, and *Globorotalia menardii* collected throughout the upper 100 m of Cariaco Basin. Plankton tows were paired with in situ measurements of water column chemistry and hydrography. The Mg/Ca ratio reflects different calcification temperatures in all three species when calculated using species-specific temperature relationships from single-species averages of Mg/Ca. However, individual shell Mg/Ca often results in unrealistic temperate estimates. The Sr/Ca ratios are relatively constant among the four species. Ratios of Mn/Ca and Ba/Ca are highest in *G. menardii* and are not reflective of elemental concentrations in open waters. The Mn/Ca ratio is elevated in all species during upwelling conditions, and a similar trend is demonstrated in *Neogloboquadrina incompta* shells from the California margin collected during upwelling periods. Together this suggests that elevated shell Mn/Ca may act as a tracer for upwelling of deeper water masses. Our results emphasize the large degree of trace element variability present among and within species living within a limited depth habitat and the roles of biology, calcification environment, and physical mixing in mediating how trace element geochemistry reflects environmental variability in the surface ocean.

INTRODUCTION

The trace elemental composition of planktic foraminiferal shells often reflects their calcification environment and is widely used for generating paleoceanographic proxy records (see Katz et al., 2010 and Schiebel et al., 2018 for reviews). Studies of foraminifera from modern environments are critical for the development, ground truthing, and calibration of these geochemical proxies. In particular, time series of trace element (TE) chemistry from foraminifera recovered from plankton tows and sediment traps have been used to determine the capabilities and limitations of TE proxies (i.e., Anand et al., 2003; McConnell & Thunell, 2005; Henehan et al., 2015) and to examine relationships between TE and ecological and biological drivers (Babila et al., 2014; Salmon et al., 2016). Such modern studies are especially valuable in regions that experience high-frequency environmental variability that can influence foraminiferal geochemistry on annual and sub-annual timescales.

High-resolution analytical techniques, such as laser ablation (LA) ICP-MS and electron microprobe analyses, are increasingly used in paleoceanographic studies. The TE/Ca ratios of individual shells, commonly referred to as individual foraminifer analyses (IFA), are now used to interpret high-frequency variability in the fossil record associated with the El Niño Southern Oscillation (Ford et al., 2015), mesoscale physical oceanographic features (Steinhardt et al., 2014), and melt-water events (Vetter et al., 2017). At the same time, these techniques have identified significant intra-shell and inter-individual TE variability for many species relevant to paleoceanography (Eggins et al., 2004; Sadekov et al., 2008; Dueñas-Bohórquez et al., 2011; Haarmann et al., 2011; Spero et al., 2015). Heterogeneity in Mg/Ca between individuals has been particularly well documented (Eggins et al., 2004; Sadekov et al., 2008; Dueñas-Bohórquez et al., 2011; Haarmann et al., 2011; Spero et al., 2015), with a lesser degree of heterogeneity demonstrated in Sr/Ca (Anand & Elderfield, 2005; Dueñas-Bohórquez et al., 2011) and in Mn/Ca (Steinhardt et al., 2014). Documenting modern variability across species and elements of interest, and identifying environmental or ecological drivers of inter-individual heterogeneity has the potential to improve and support paleoceanographic interpretations.

This study compares inter-individual and inter-species TE/Ca heterogeneity in three species of planktic foraminifera frequently used in paleoceanographic reconstructions, *Globigerina ruber* (pink) (d'Orbigny, 1839), *Orbulina universa* (d'Orbigny, 1839), and *Globorotalia menardii* (Parker, Jones & Brady, 1865), collected by plankton tow in the Cariaco Basin, off the coast of Venezuela. The temporal variability in foraminiferal Mg/Ca, Sr/Ca, Ba/Ca, and Mn/Ca is compared to in situ hydrological and chemical water column measurements, and the association of these trace elements with physical mixing processes in Cariaco Basin is explored.

SETTING

Cariaco Basin

The Cariaco Basin is located off the coast of Venezuela, and is home to the long-term CARIACO time series program (Muller-Karger et al., 2019). High productivity and a long observational time series of water column properties make it an excellent location for studying the associations between planktic foraminifera and their environment. The Cariaco Basin is a deep (1400 m) basin, isolated from the

---

[1] School of the Earth, Ocean, and Environment, University of South Carolina, Columbia, SC, 29208

[2] Present Address: Department of Geology and Geophysics, Yale University, New Haven, CT 06511

[3] College of Earth, Ocean, and Atmospheric Science, Oregon State University, Corvallis, OR, 97301

[†] Deceased July 30, 2018

[*] Correspondence author. E-mail: cvdavis@seoe.sc.edu

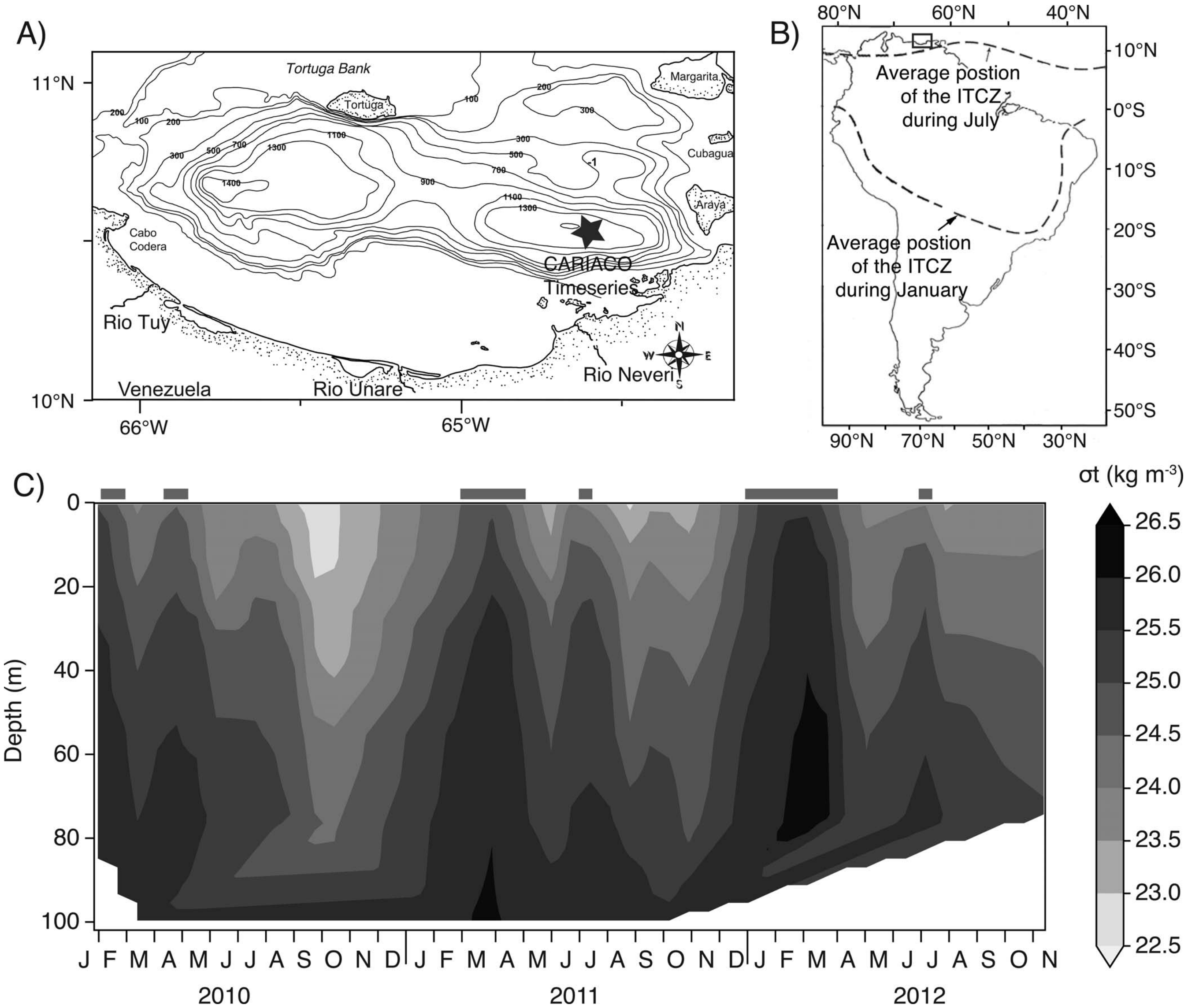

FIGURE 1. A) The location of the CARIACO time series station in the Cariaco Basin (star), off of the Venezuela coast; B) broader view showing the seasonal migration of the ITCZ about the equator, with the location of the Cariaco Basin shown as a box; and C) a time series of σt at the CARIACO time series station, interpolated between monthly CTD casts for the study period. Periods designated as upwelling are marked by gray boxes.

Caribbean Sea by a shallow ~140 m sill to the north. As a result of limited ventilation below the sill, the deep basin is anoxic, with the oxic/anoxic boundary generally found 250–350 m deep (Scranton et al., 2014). The resulting preservation of sediments has made the basin an important archive of past climate fluctuations (e.g., Peterson et al., 1991; Lin et al., 1997; Haug et al., 2001; Tedesco & Thunell, 2003a; Black et al., 2007).

Each year the Intertropical Convergence Zone (ITCZ) migrates southward during the winter, driving strong easterly trade winds that promote upwelling in Cariaco Basin (Fig. 1). The ITCZ migration typically begins in November–December and lasts until April–May. It is accompanied by shoaling of isotherms in the upper 150 m and a slight increase in sea surface salinity (Muller-Karger et al., 2001, 2019; Astor et al., 2003). A short, secondary period of upwelling is commonly observed between June and August (Astor et al., 2003). Upwelling of nutrient rich deep waters drives a seasonal increase in primary productivity and mass flux to depth (Thunell et al., 2000; Muller-Karger et al., 2001; Goni et al., 2003; Scranton et al., 2006). Summer brings a substantial increase in rainfall and thus riverine and terrestrial inputs to the Cariaco Basin from the *Manzanares*, *Neveri*, *Unare*, and *Tuy* rivers, and a decrease in sea surface salinity at the study site (Lorenzoni, 2005; Lorenzoni et al., 2009; McConnell et al., 2009).

Species

The three species investigated in this study, *Globigerina ruber* (pink), *Orbulina universa*, and *Globorotalia menardii* are present year-round in the basin with somewhat higher abundances associated with periods of upwelling (Tedesco et al., 2007). Both *G. ruber* (pink) and *O. universa* are spinose and harbor dinoflagellate symbionts, while *G. menardii* lacks spines and contains intracellular algal symbionts (Gastrich, 1987; Hemleben et al., 1989; Gast & Caron, 1996; Shaked & de Vargas, 2006; Schiebel & Hemleben, 2017). Oxygen isotope values show that *G. ruber* (pink and white) calcifies within the upper 25 m of the water column in Cariaco Basin, while *O. universa* and *G. menardii* occupy a deeper and wider range of depths. *Globorotalia menardii* calcifies at a depth range between 25 and 200 m in this region (Tedesco et al., 2007; Wejnert et al., 2013) whereas *O. universa* calcifies shallower, between 25 and 150 m and has been shown to undergo seasonal vertical migrations that follow the 19–22°C isotherms (Tedesco et al., 2007). The range of calcification depths reported for these species are similar throughout the Caribbean (e.g., Jones, 1968; Steph et al., 2009; Jensen et al., 2018a), however we rely most heavily on local results given the presence of seasonal upwelling and relatively shallow oxycline specific to the Cariaco Basin.

METHODS

Plankton Tows

Integrated vertical plankton tows (200-μm mesh) from 100 m depth to the surface were collected monthly in the Cariaco Basin at the CARIACO time series station (10°30'N; 64°40'W) between January 2010 and November 2012 (n = 30) onboard the R/V *Hermano Gines* (Fig. 1). A Conductivity-Temperature-Depth (CTD) profile (SeaBird Scientific model 25) and discrete bottle sampling at multiple depths accompanied each plankton tow. A full account of the methods used for in situ and discrete sampling as a part of the CARIACO time series can be found in the CARIACO Methods Manual (http://imars.marine.usf.edu/sites/default/files/project/cariaco/publications/CARIACO_Methods_Manual.pdf). Plankton tow material was preserved shipboard in formalin buffered with sodium borate. For comparison purposes, we include trace element data from the planktic species *Neogloboquadrina incompta* (Cifelli, 1961) collected from plankton tows (150-μm mesh) on the Central California Margin (38.3°N; 123.0°W) in November 2012 and June 2014 onboard the R/V *Mussel Point*.

Sample Preparation and Cleaning

Cariaco Basin plankton tow material was washed over a 200-μm sieve and foraminifera were removed and dried; shells of *G. ruber* (pink), *O. universa*, and *G. menardii* were picked for further analyses. *Neogloboquadrina incompta* shells were wet picked from tows, rinsed in de-ionized water, and stored without preservatives in micropaleontology slides. Several specimens from the Cariaco Basin were mounted on carbon tape and gold sputter coated for Scanning Electron Microscope (SEM) imaging. Imaging was carried out on a Tescan Vega3 SEM in the Electron Microscopy Center at the University of South Carolina (Appendix Fig. S1). All remaining foraminifera from both the Cariaco Basin and the California Margin were subjected to an oxidative cleaning process to remove organic material as previously described for cultured foraminifera (Mashiotta et al., 1999). Briefly, foraminifera were immersed in a 1:1 solution of 0.1N NaOH and 30% H_2O_2 heated to ~65°C for 10 minutes during which they were ultrasonicated for four 10-s periods at 2.5-minute intervals, then rinsed twice in ultrapure water. Between 1 and 23 individuals from each population were then analyzed by LA ICP-MS (Appendix Table S1).

ICP-MS Methods

Cleaned foraminifera were mounted on carbon tape and analyzed using a Photon Machines 193 nm ArF laser with an ANU HelEx dual-volume laser ablation cell coupled to a Thermo Finnegan Element 2 ICP-MS at the University of South Carolina. A 65-μm circular spot size was used to analyze each chamber of the final whorl from the outside-in with 1–3 analyses per chamber. Individual spots were ablated using a 3-Hz repetition rate and a fluence of 2 J cm^{-2}. Ablated material was transported in a He-Ar gas mixture through a 'squid', with flow rate tuned daily between 0.71 and 1 L min^{-1}. Isotopes of ^{25}Mg, ^{43}Ca, ^{55}Mn, ^{87}Sr, and ^{137}Ba, were analyzed by laser ablation in Escan mode, with a sample time of 10 ms for each analyte. We used NIST SRM 610 and 612 glasses for reference materials with compositional values from Jochum et al. (2011), which were analyzed between every ~10 shells to correct for drift. At the beginning of each LA ICP-MS session, the final chamber of a single *G. menardii* shell was analyzed for a total of 10 repeat measurements. The standard deviation (σ) of repeat measurements of the profile average was 0.1 mmol/mol for Mg/Ca, <0.0 mmol/mol for Sr/Ca, 8.9 μmol/mol for Mn/Ca, and 3.3 μmol/mol for Ba/Ca. Data reduction was carried out using the LATools software (Branson et al., 2019). Where multiple ablations were possible in a chamber, these were averaged for a single chamber TE/Ca ratio. Unless otherwise specified, TE ratios refer to the mean of all chambers ablated in an individual shell, such that the TE/Ca of all chambers are equally weighted. Samples of California Current *N. incompta* from an upwelling (n = 20) and non-upwelling interval (n = 11), initially analyzed for a different project, were pooled, dissolved in 1% nitric acid, and analyzed on the same Thermo Finnegan Element 2 ICP-MS. Due to slight differences in analytical methodology, these samples are compared only to one another and not quantitatively to laser-ablated Cariaco Basin samples.

RESULTS

Trace Element Heterogeneity Between Species

Globogerinoides ruber (pink), *Orbulina universa*, and *Globorotalia menardii* all have significantly different TE compositions from one another (Wilcox Rank Sum test with Bonferroni correction; all $p < 0.05$). *Orbulina universa* has the highest Mg/Ca ratio (mean = 12.2 mmol/mol, sd = 2.7 mmol/mol), followed by *G. ruber* (pink) (mean = 5.9 mmol/mol, sd = 1.7 mmol/mol), with *G. menardii* having the lowest values (mean = 3.2 mmol/mol, sd = 1.1 mmol/mol). *Globigerinoides ruber* (pink) has the highest Sr/Ca ratio (mean = 1.6 mmol/mol, sd = 0.1 mmol/mol), followed by *G. menardii* (mean = 1.5 mmol/mol,

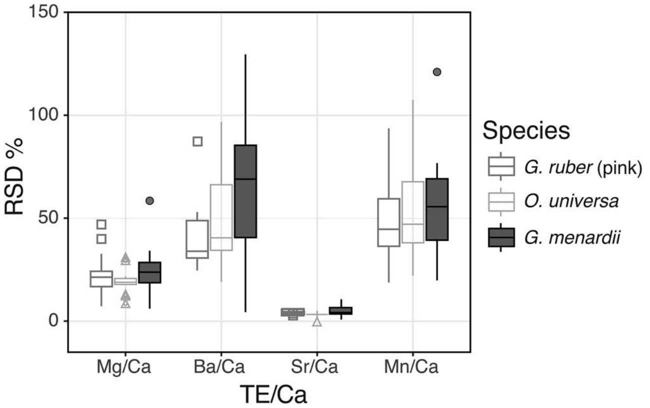

FIGURE 2. Boxplot showing the relative standard deviations (RSDs) of Ba/Ca, Mg/Ca, Mn/Ca, and Sr/Ca ratios in individual *G. ruber*, *O. universa*, and *G. menardii* for all tows. Horizontal bars represent the median, and boxplot bounds the 1st and 3rd quartile.

sd = 0.1 mmol/mol) and then *O. universa* (mean = 1.5 mmol/mol, sd = 0.1 mmol/mol). *Globorotalia menardii* has both the highest Mn/Ca and Ba/Ca ratios (means = 87.8 and 14.6 μmol/mol, sd = 55.1 μmol/mol and 15.0, respectively), followed by *G. ruber* (pink) (means = 16.4 and 7.1 μmol/mol, sd = 13.1 and 4.8 μmol/mol, respectively) and *O. universa* (means = 11.4 and 5.4 μmol/mol, sd = 9.9 and 3.9 μmol/mol, respectively).

TRACE ELEMENT HETEROGENEITY BETWEEN INDIVIDUALS

The degree of inter-individual variability found within each population, defined as individuals of the same species retrieved in a single plankton tow, varies by both species and TE (Fig. 2). Within a population, inter-individual heterogeneity can be expressed by the standard deviation relative to the mean (RSD%). Within a population, Sr/Ca RSD is lowest in all species, ranging between 0.01% and 9.9% in *G. menardii* (mean = 5.0%), between 3.3% and 8.4% in *G. ruber* (mean = 4.8%), and is especially low in *O. universa* at just 0.2% to 5.8% (mean = 3.4%). The Mg/Ca RSDs are higher, ranging between 5.4% and 57.7% in *G. menardii* (mean = 23.8%), between 7.3% and 47.0% in *G. ruber* (mean = 23.2%), and still lowest in *O. universa*, between 8.7% and 31.1% (mean = 20.3%). The RSD of both Ba/Ca and Mn/Ca is much higher, with values exceeding 100% in some populations. For Ba/Ca, RSDs range between 3.7% and 129.8% in *G. menardii* (mean = 72.0%), 24.7% to 87.4% in *G. ruber* (mean = 40.0%), and 19.2% to 96.8% in *O. universa* (mean = 46.3%). The Mn/Ca RSDs ranged from 19.1% to 120.2% in *G. menardii* (mean = 52.3%), 18.8% to 93.7% in *G. ruber* (mean = 48.0%), and 22.2% to 107.8% in *O. universa* (mean = 50.9%). Thus, the highest RSDs in all TE are consistently observed in *G. menardii* (Fig. 2).

Since variables including temperature, salinity, and pH covary with one another and with density, we used the density gradient of the water column between 100 m and the surface as an approximation of the range of environmental conditions foraminifera could have been exposed to during each tow (Appendix Fig. S2). This approach allows us to minimize assumptions about which combination of environmental variables drive TE compositions. The results indicate that although higher RSDs are sometimes associated with greater variability in the water column, this is neither universal nor sufficient to explain the degree of population diversity observed.

Ontogenetic Influence on Trace Elements

A repeated measure ANOVA that accounts for individual foraminifera was carried out on angularly transformed TE/Ca data (accounting for non-normality) to test for variability between successive chambers in *G. ruber* (pink) and *G. menardii* (Figure 3). Chamber-to-chamber variability was significant in both species for Mg/Ca [*G. ruber* (pink): F(1, 212) = 153.7, $p < 0.005$; *G. menardii*: F(1, 128) = 20.9, $p < 0.005$], Sr/Ca [*G. ruber* (pink): F(1, 212) = 38.2, $p < 0.005$; *G. menardii*: F(1, 128) = 70.7, $p < 0.005$], and Mn/Ca [*G. ruber* (pink): F(1, 203) = 130.4, $p < 0.005$; *G. menardii*: F(1, 121) = 7.2, $p = 0.008$]. For Ba/Ca [F(1, 210) = 173.5, $p < 0.005$], significant differences only occurred in *G. ruber* (pink) (Table 1). The trend is also generally different between the two species. The ratios of Mg/Ca, Sr/Ca, Ba/Ca, and Mn/Ca all decrease in successive (from older to younger) chambers of *G. ruber* (pink). In *G. menardii*, while both Mg/Ca and Sr/Ca increase in successive chambers, Mn/Ca decreases (Fig. 3). Most, although not all, individual foraminiferal analyses follow these trends, with 83% of *G. ruber* (pink) (n = 213) showing a decrease in Mg/Ca in subsequent chambers and 59% a decrease in Sr/Ca. In *G. menardii* (n = 127), 57% show an increase in Mg/Ca and 79% an increase in Sr/Ca. In all, 80% of *G. ruber* (pink) and 59% of *G. menardii* decrease in Mn/Ca, and 90% of *G. ruber* (pink) decrease in Ba/Ca.

TEMPORAL VARIABILITY IN TRACE ELEMENT RATIOS

Mg/Ca Ratio and Implied Calcification Temperatures

The Mg/Ca ratios ranged from 2.6 to 17.7 mmol/mol in *G. ruber* (pink), 5.5 to 21.9 mmol/mol in *O. universa*, and 1.7 to 8.5 mmol/mol in *G. menardii*. We compared the species-specific Mg/Ca:temperature relationships previously established for all three species. Several relationships specific to *G. ruber* (white) were also tested for *G. ruber* (pink) (Dekens et al., 2002; McConnell & Thunell, 2005; Regenberg et al., 2009; Gray et al., 2018) as were multi-species relationships (Anand et al., 2003; Elderfield & Ganssen, 2000; Appendix Fig. S3). Of the published relationships for both white and pink *G. ruber*, the relationship from Gray et al. (2018), which includes salinity and pH (from the shallowest 1 m bin), yields temperatures closest to measured surface temperatures at the study location at the time of collection. Most other relationships, however, result in warmer than observed temperatures (Appendix Fig. S3). For *O. universa*, the species-specific Lea et al. (1999) relationship gave reasonable calcification temperatures, as did the Gray et al. (2019) relationship inclusive of salinity and pH at 35 m (Appendix Fig. S3). When applied to Mg/Ca ratios in *G. menardii*, the Regenberg et al. (2009) and Anand et al. (2003) relationships reflect temperatures around 100 m whereas other relationships would place this species far below the 100 m tow depth in the water column (Fig. 4).

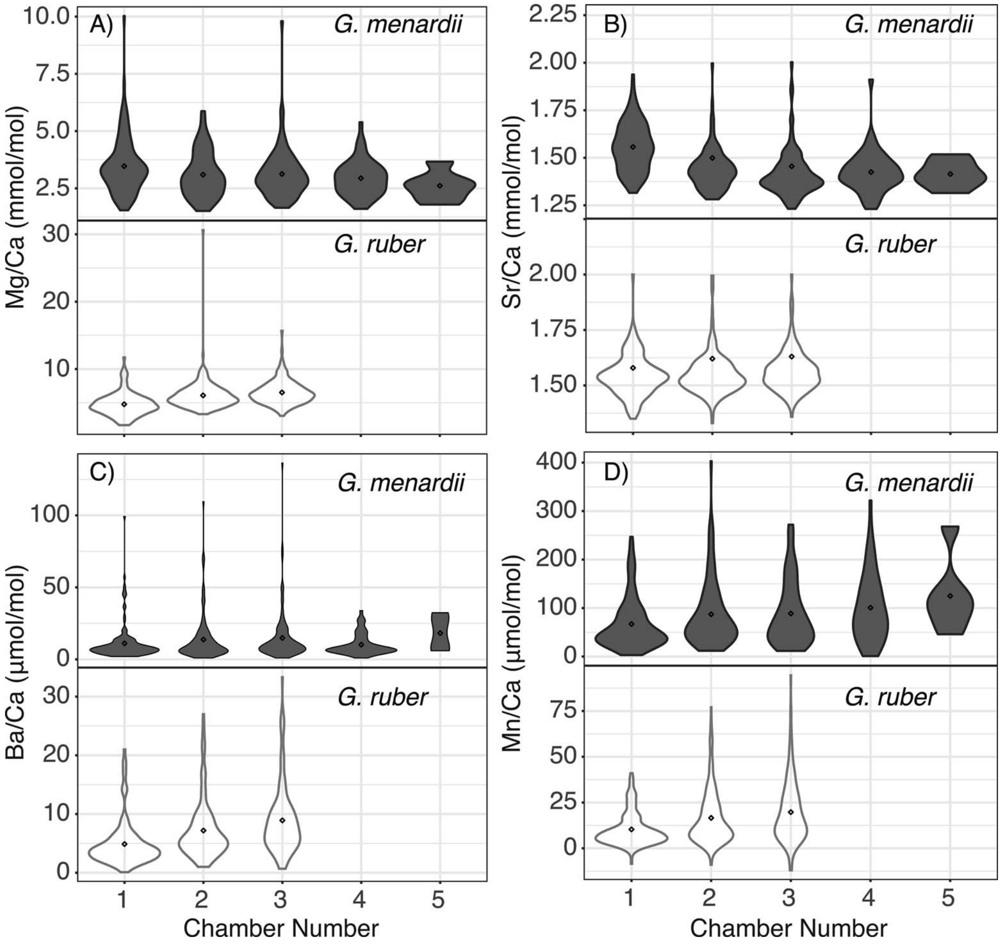

FIGURE 3. Violin plots of individual chamber average measurements in *G. menardii* and *G. ruber* for A) Mg/Ca; B) Sr/Ca; C) Mn/Ca; and D) Ba/Ca. Means are shown as black points.

The average Mg/Ca ratio of populations represented by at least 10 individuals yields reasonable (within 3°C) approximations of temperature measured at the surface (1 m) for *G. ruber* (pink) and 35 m for *O. universa* or within 6°C of temperature at 100 m for *G. menardii* when the most appropriate equations are applied (Fig. 4A). However, individual shell Mg/Ca ratios produce an unrealistic range of calcification temperatures for the upper 100 m of the water column (Fig. 4B). For example, in the most Mg/Ca-variable population for each species, Mg/Ca ratios from individual shells would suggest temperatures ranging between 16–29°C in *O. universa* from the collection on August 4th, 2010 compared to a 22–28°C range actually measured in the water column. In *G. ruber* (pink), a range of 22–39°C is calculated by the Mg/Ca ratio of individuals collected on September 15th, 2010, in contrast to the 24–30°C measured in the water column. In *G. menardii*, temperatures between 20–35°C were inferred from shells collected on January 10, 2012, while water column temperatures were measured between 20–25°C.

We also assessed Mg/Ca variability in association with upwelling conditions, defined as periods when CTD data indicates that sigma-t (σt) at 25 m exceeds 25 kg m^{-3} (Fig. 1). To compare populations for the two conditions (upwelling vs. non-upwelling), we used a Kruskal-Wallis test, which accounts for the inherent potential for non-normal population distributions of TE data normalized to Ca. In comparing upwelling and non-upwelling conditions, Mg/Ca ratios were significantly lower in *G. ruber* (pink) (Chi squared = 6, p = 0.01, df = 1), higher for *O. universa* (Chi squared = 5.4, p = 0.01, df = 1), and not significantly different for *G. menardii* (p = 0.3) (Fig. 5A).

Sr/Ca Ratio

Ratios of Sr/Ca ranged between 1.3 and 2.0 mmol/mol in *G. ruber* (pink), 1.3 and 1.7 mmol/mol in *O. universa*, and 1.3 and 1.9 mmol/mol in *G. menardii*; these ratios are the least variable of the four elements analyzed. Ratios of Sr/Ca are lower in *G. ruber* (pink) during upwelling conditions (Chi squared = 8.2, p = 0.004, df = 1), higher overall in *G. menardii* (Chi squared = 6.5, p = 0.01, df = 1), and not significantly different in *O. universa* (Chi squared = 3.3, p = 0.07, df = 1) (Fig. 5B).

Mn/Ca Ratio

Ratios of Mn/Ca ranged between 0.6 and 78.1 µmol/mol in *G. ruber* (pink), 0.3 and 67.7 µmol/mol in *O. universa*, and

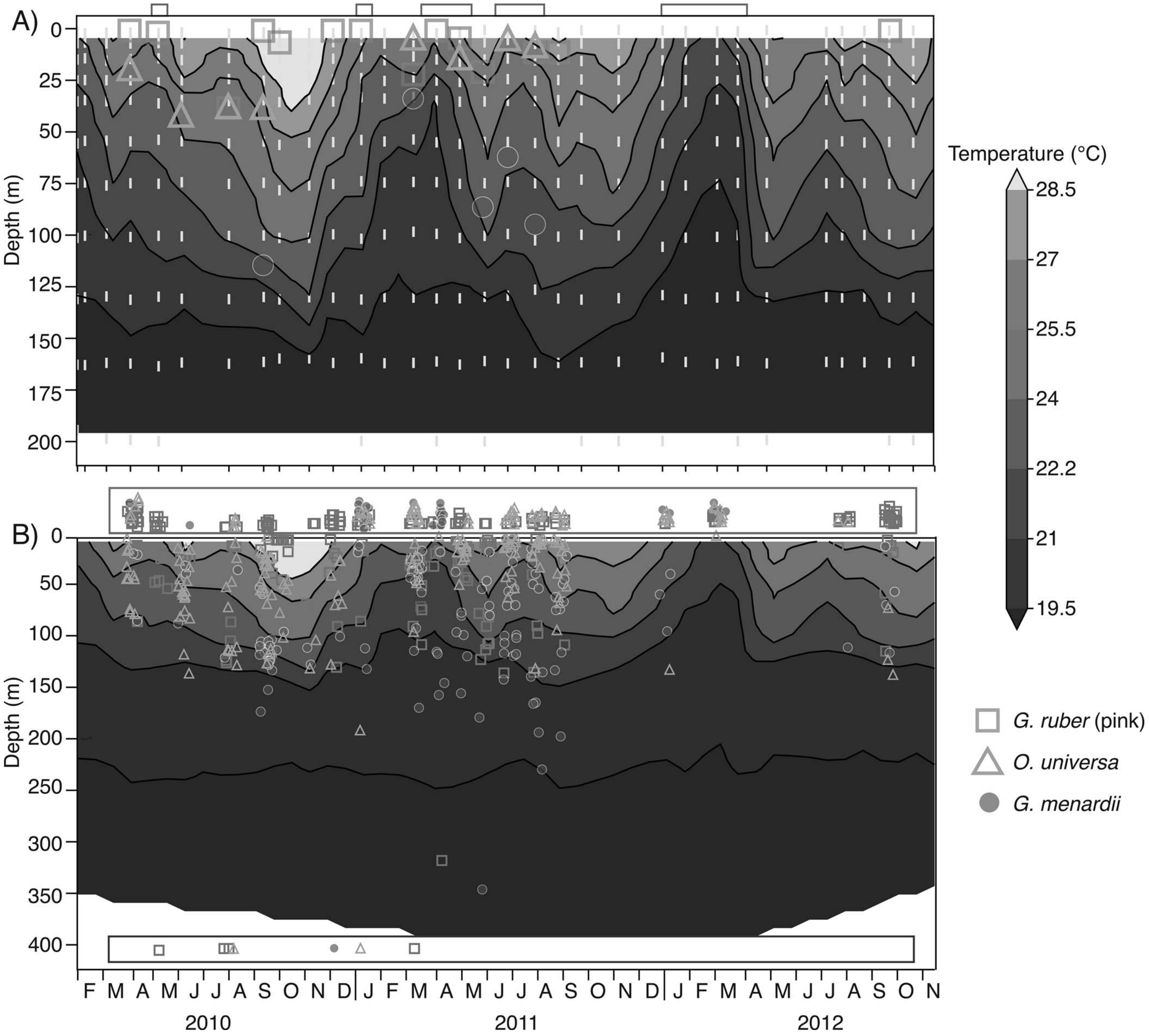

FIGURE 4. Interpolated time series of temperature from monthly CTD casts (dashes) with upwelling periods shown as gray bars above, A) calcification depth implied by Mg/Ca ratios from populations represented by more than 10 individuals; and B) calcification depth implied by Mg/Ca ratios of individuals. Individuals representing temperatures outside the range measured in the upper 400 m of the water column on the day that they were collected are shown are shown above if warmer or below if cooler. Temperatures are derived using the equations of Gray et al. (2018) for *G. ruber*, Lea et al. (1999) for *O. universa*, and Regenberg et al. (2009) for *G. menardii*. Points have been jittered, randomly distributed in the x-dimension within each bin, to increase visibility.

15.7 and 243.0 μmol/mol in *G. menardii*. Upwelling conditions are associated with higher Mn/Ca for all three species: *G. menardii* (Chi squared = 11.5, $p < 0.001$, df = 1), *O. universa* (Chi squared = 62.5, $p < 0.001$, df = 1), and *G. ruber* (pink) (Chi squared = 7.8, p = 0.005, df = 1) (Fig. 5C).

Ba/Ca Ratio

Ratios of Ba/Ca ranged between 1.0 and 33.3 μmol/mol in *G. ruber* (pink), 0.5 and 27.0 μmol/mol in *O. universa*, and 1.0 and 83.5 μmol/mol in *G. menardii*. Upwelling conditions are associated with higher Ba/Ca in *G. ruber* (pink) (Chi squared = 4.2, p = 0.04, df = 1), and *O. universa* (Chi squared = 13.4, p = 0.002, df = 1), but are not significantly different in *G. menardii* (p = 0.49) (Fig. 5D). To explore potential environmental associations with foraminiferal Ba/Ca, we compare Ba/Ca ratios to sea surface salinity as a metric of riverine inputs (e.g., Weldeab et al., 2007; Bahr et al., 2013; Evans et al., 2015; Vetter et al., 2017), chlorophyll *a* in the upper 100 m as a metric of productivity, and covariance with elevated Sr/Ca in shells as a potential indicator of exposure to acantharian blooms.

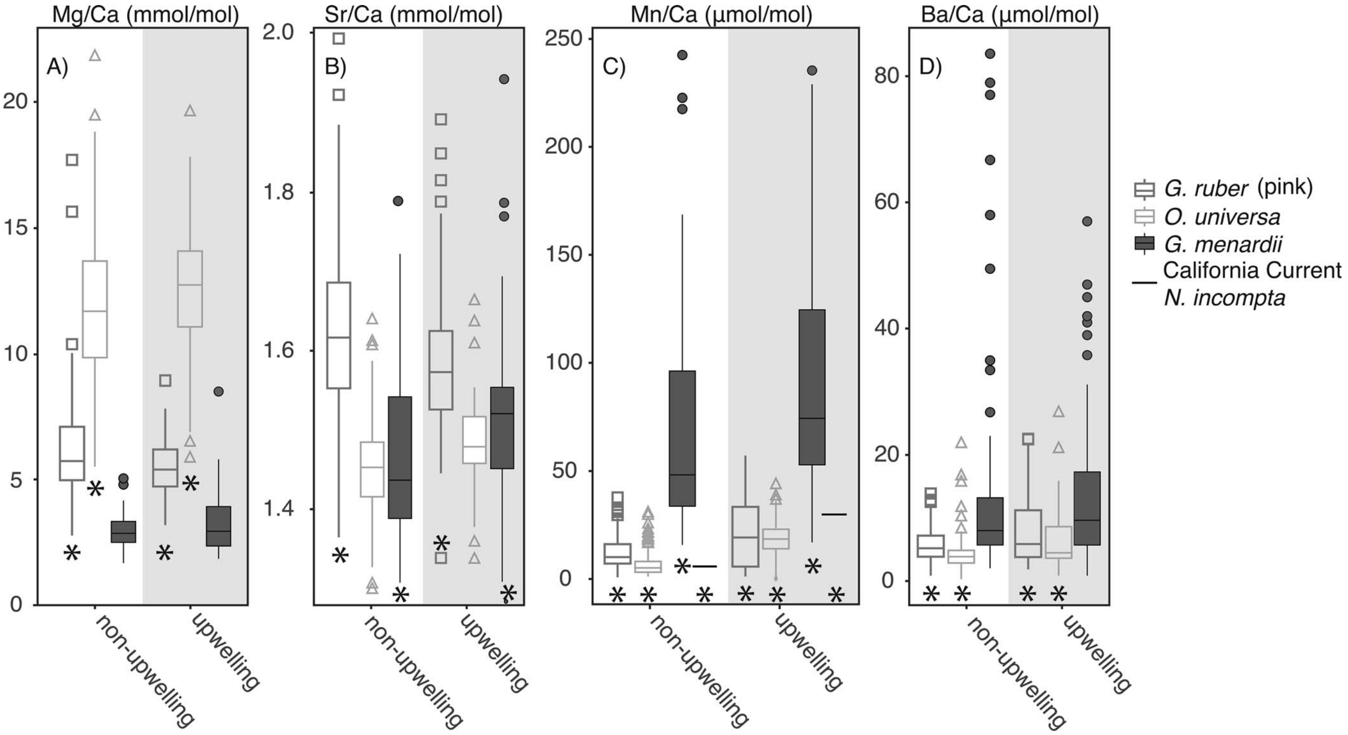

FIGURE 5. Boxplots of A) Mg/Ca; B) Sr/Ca; C) Mn/Ca; and D) Ba/Ca ratios in *G. ruber*, *O. universa*, and *G. menardii* collected during upwelling compared to non-upwelling conditions. Asterisks are shown below populations with are significantly different during upwelling versus non-upwelling conditions. Horizontal bars represent the median, and boxplot bounds the 1st and 3rd quartile.

Based on a simple linear regression against individual shell values, salinity was not a significant predictor of Ba/Ca in any species ($p > 0.05$). In contrast, chlorophyll *a* integrated over the upper 100 m, explained a small but significant component of individual shell Ba/Ca in *G. ruber* (pink) ($r^2 = 0.27$; $p < 0.001$) and *O. universa* ($r^2 = 0.13$; $p < 0.001$), but not in *G. menardii* ($r^2 < 0.00$; $p = 0.01$). Testing for the presence of high Sr/Ca in the same shells as elevated Ba/Ca yielded no significant correlation ($p > 0.05$) in either *G. ruber* (pink) or *O. universa* and only a weak correlation in *G. menardii* (0.16, $p = 0.04$).

TE AND SHELL SIZE VARIABILITY

To test for correlations between TEs and shell size (measured on the longest dimension), we used a Kendall partial correlation test, while controlling for individual tow. Shell size has a significant positive correlation with Mg/Ca in *O. universa* and *G. ruber* (pink) (0.11, $p = 0.01$ and 0.1, $p = 0.05$, respectively), but not in *G. menardii* (0.04, $p = 0.43$). For Sr/Ca, a significant negative correlation was found in *G. menardii* (−0.20, $p = 0.004$) but not in *O. universa* and *G. ruber* (pink) (0.02, $p = 0.70$ and 0.00, $p = 0.96$, respectively) (Fig. 6). Neither Mn/Ca nor Ba/Ca had any correlation with size in *O. universa* (0.05, $p = 0.31$; 0.07, $p = 0.13$), *G. ruber* (pink) (−0.08, $p = 0.10$; −0.03, $p = 0.39$), or *G. menardii* (−0.08, $p = 0.34$; −0.05, $p = 0.39$). Shells of *O. universa* are found to be smaller overall during upwelling (Chi squared = 10.2, $p = 0.001$, df = 1), but not *G. ruber* (pink) ($p = 0.07$), or *G. menardii* ($p = 0.51$).

DISCUSSION

HETEROGENEITY IN INDIVIDUAL TRACE ELEMENT RATIOS

Significant inter-individual heterogeneity among specimens in Mg/Ca and Sr/Ca has previously been identified in core tops (Anand & Elderfield, 2005; Sadekov et al., 2008) as well as in culture-grown foraminifera where environmental variables (e.g., T, S, pH) are controlled (Dueñas-Bohórquez et al., 2011; Spero et al., 2015; Davis et al., 2017). Since our analyses were carried out on plankton tow specimens, individual TE variability reflects a combination of differing habitats within the water column (limited by tow depth from 0 to 100 m) and species-specific vital effects, including ontogenetic stage, varying uptake of TE during calcification, and potentially inter-chamber variability in the cases of *G. ruber* (pink) and *G. menardii*, but limited temporal variability.

Previous studies have identified higher Mg/Ca variance relative to Sr/Ca in individuals of the species *Globigerina bulloides* (d'Orbigny, 1826), *Trilobatus sacculifer* (Brady, 1877), and *Globorotalia truncatulinoides* (d'Orbigny, 1839) (Anand & Elderfield, 2005; Dueñas-Bohórquez et al., 2011). We also find Sr/Ca to be the least variable of the Te/Ca ratios measured in *G. ruber* (pink), *O. universa*, and *G. menardii* (Figs. 2, 5). This is followed by Mg/Ca; both Ba/Ca and Mn/Ca were more variable among individuals from a single tow (Figs. 2, S4). It is likely that foraminifera exhibit tighter biological control over the incorporation of Mg and Sr, in contrast to Ba or Mn, which are incorporated into foraminiferal shells in proportion to their concentration in the immediate calcification environment (Munsel et al., 2010; Hönisch

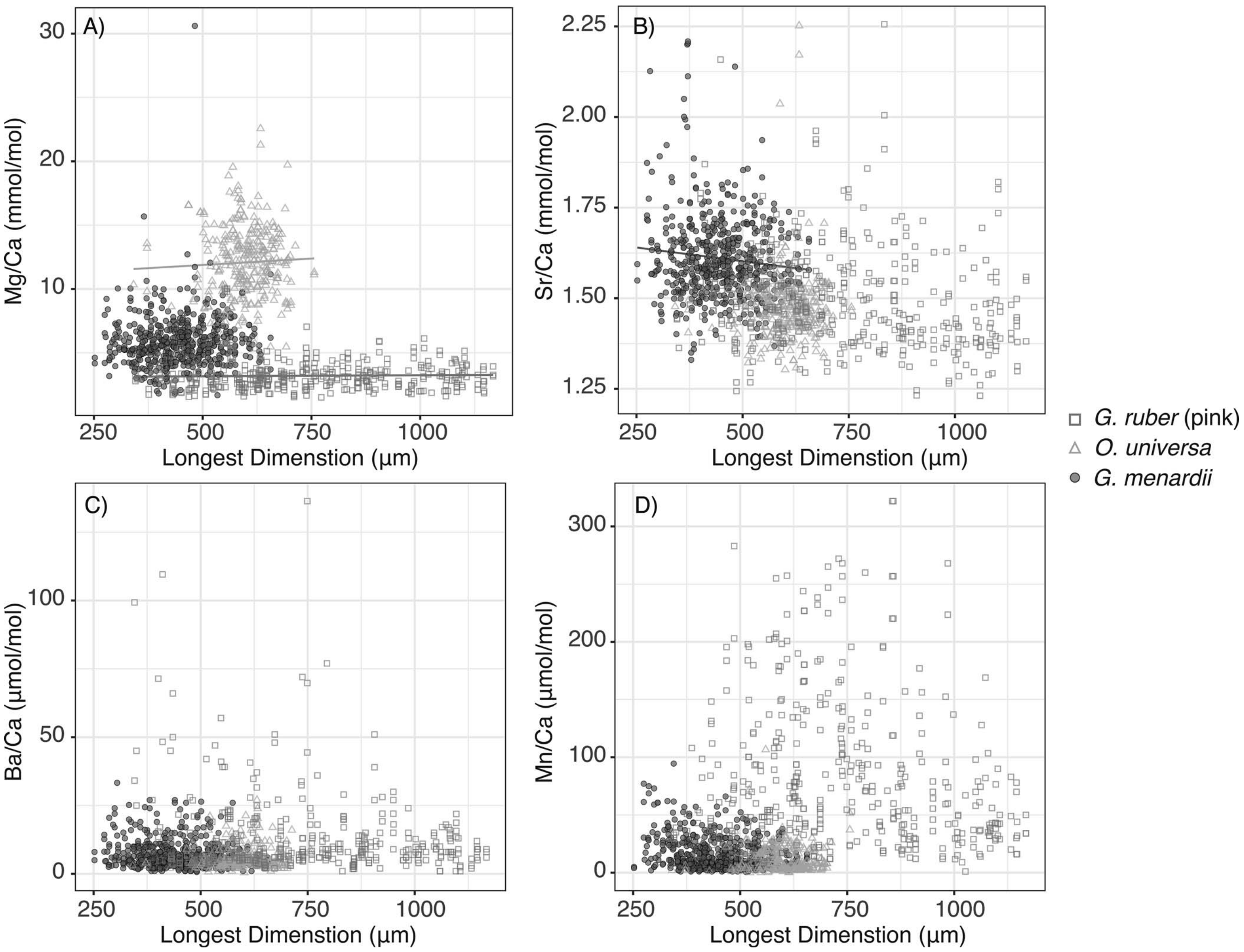

FIGURE 6. Cross plots of A) Mg/Ca; B) Sr/Ca; C) Ba/Ca; and D) Mn/Ca with shell size, measured by the longest dimension, for *G. ruber*, *O. universa*, and *G. menardii*. Linear regression lines are shown for species where a significant relationship was determined between TE composition and size.

et al., 2011; Barra et al., 2018; van Dijk et al., 2019; Fehrenbacher et al., 2018). Trace element to calcium ratios within *G. menardii* were also more variable than in *O. universa* and *G. ruber* (pink) (Figs. 2, S4). This could result from a wider range of habitat depths or a more variable microenvironment not reflective of open seawater, such as a marine snow substrate as suggested for *N. dutertrei* (Fehrenbacher et al., 2018). Moreover, analyses of *O. universa* were carried out only on the terminal, spherical chamber, limiting the potential for ontogenetic effects in comparison to the other two species.

ONTOGENETIC TRENDS IN TRACE ELEMENT INCORPORATION

Previous work has demonstrated ontogenetic controls on TE/Ca ratios in several extant species of planktic foraminifera with outcomes of decreasing, increasing, or no systematic change in the Mg/Ca of progressively younger chambers, as summarized in Table 1. Fewer studies have looked at inter-chamber variability in other elements. For example, studies of individual chamber Sr/Ca and Mn/Ca found no significant chamber-to-chamber difference in Sr/Ca (Anand & Elderfield, 2005; Dueñas-Bohórquez et al., 2011) and a decrease in Mn/Ca in progressively younger chambers (Steinhardt et al., 2014). Our data along with other existing work shows that Mg/Ca ratios appear to decrease in younger chambers across most spinose species, but increase in younger chambers of non-spinose species (Table 1). The divergence between spinose and non-spinose species may be due to a low-Mg crust found in several non-spinose species, including *N. dutertrei* and *G. truncatulinoides*, which decreases in thickness in younger chambers (Steinhardt et al., 2015; Fehrenbacher et al., 2017). The same may be the case for crusted *G. menardii* (Table 1).

Given that chamber-to-chamber differences in Mg/Ca have also been observed in cultured foraminifera, it is unlikely that macroenvironmental variables or migration in the water column are the sole drivers of inter-chamber TE/Ca variability (e.g., Dueñas-Bohórquez et al., 2011). Chamber-to-chamber differences in Mg/Ca from multiple studies of

TABLE 1. Summary of published finds on systematic inter-chamber trends from oldest to youngest chambers in planktic foraminiferal Mg/Ca, Sr/Ca, Mn/Ca and Ba/Ca ratios. New results from this study for G. menardii and G. ruber (pink) are included in the first two rows.

Species	Mg/Ca	Sr/Ca	Mn/Ca	Ba/Ca	Study
G. menardii	Increase	Increase	Decrease	- -	This study; Jochum et al. (2019)
G. ruber (pink)	Decrease	Decrease	Decrease	Decrease	This study
G. ruber (white)	- -		Decrease		Steinhardt et al. (2014)
G. ruber (white)	- -				Sadekov et al. (2008)
G. ruber (white)	Decrease (in F only)				Bolton (2011)
G. ruber (white)	Decrease (in F only)				Wit et al. (2010)
G. bulloides	Decrease	- -			Anand & Elderfield (2005)
G. bulloides	Decrease				Marr et al. (2011)
G. sacculifer	Decrease	- -			Duenas-Bohorquez et al. (2011); Jentzen et al. (2018
G. scitula	- -		Decrease		Steinhardt et al. (2014)
G. truncatulanoides	Increase	- -			Anand & Elderfield (2005)
N. dutertrei	Increase		- -	- -	Steinhardt et al. (2014); Fehrenbacher et al. (2018)
N. incompta	- -				Davis et al. (2017)
N. incompta	- -				Bolton (2011)
N. pachyderma	- -				Davis et al. (2017)
P. obliquiloculata	- -		- -		Steinhardt et al. (2014)

G. bulloides (Anand & Elderfield, 2005; Marr et al., 2011) and *T. sacculifer* (Sadekov et al., 2005; Duenas-Bohorquez et al., 2011; Jentzen et al., 2018b) consistently show a decrease in ratio with ontogeny, however in *G. ruber* (white), authors have alternatively found either a decrease from the penultimate to the final chamber (Wit et al., 2010; Bolton, 2011) or no change (Sadekov et al., 2008; Steinhardt et al., 2014). We note that despite clear overall chamber-to-chamber trends, there are some individuals that do not appear to follow these patterns. If ontogenetic trends in TE vary with site or through time, this would caution against comparison of long-term records based only on final chamber analyses. Although no obvious environmental drivers have been identified in this study that can explain either ontogenetic trends or individual outliers, further replication of results from the same species across other modern environments or within culture studies are still needed to assess whether chamber-to-chamber differences in paleoceanographically significant trace metals could be population or site specific.

SEASONALITY OF TE/CA RATIOS

Mg/Ca Ratio and Temperature

Given the wide use of Mg/Ca in planktic foraminifera as a paleothermometer, we have applied previously published Mg/Ca:temperature relationships to the Mg/Ca of each species. Reasonable temperatures at assumed depth are achieved when applying the relationship from Gray et al. (2018), inclusive of pH and temperature, to *G. ruber* (pink); the species-specific relationship from Lea et al. (1999) to *O. universa*; and the species-specific relationship from Regenberg et al. (2009) to *G. menardii*. All individuals lived in the upper 100 m (depth of plankton tow) at the time of capture, although this does not necessarily rule out the possibility that some calcite formed at greater depths. If we assume that the chosen Mg/Ca relationships approximate calcification temperature, our results validate previous observations of a year-round, near-surface habitat for *G. ruber* (pink) (Tedesco et al., 2007; Wejnert et al., 2013; Fig. 4A). For *O. universa*, species-specific average Mg/Ca temperatures imply calcification throughout the upper water column, concentrated above 50 m (Fig. 4A). Calcification temperatures for *G. menardii* suggest that captured individuals were living throughout the upper 100 m, with some calcification having occurred deeper (Fig. 4A). The likelihood of a seasonal migration to below 100 m during nonwelling explains the sporadic absence of both *O. universa* and *G. menardii* from tows, in contrast to their year-round presence in sediment traps at ~230 m (Tedesco et al., 2007; Wejnert et al., 2013), as well as the exceptionally wide range of temperatures recorded by the Mg/Ca of *G. menardii* in particular (Fig. 4).

Even taking into account the potential for migration, individual shell Mg/Ca ratios are often too great to be explained by temperature alone (Sadekov et al., 2009; Dueñas-Bohórquez et al., 2011; Spero et al., 2015). In most tows, temperature estimates from individuals (±2°C) exceed the range observed across the entire upper 100 m (Fig. 4B). Moreover, only in *G. ruber*, do RSDs of Mg/Ca within a population show an increase with an increasing environmental range within the upper water column (Figure S2), suggesting that the range of measured Mg/Ca cannot be entirely accounted for by a diversity of depth habitats. Thus, while population average Mg/Ca values are indicative of temperature, any given shell may be too heavily influenced by unconstrained microenvironmental or vital effects to offer an entirely reliable temperature estimate.

Ratios of Mg/Ca in each species in the Cariaco Basin and the contrasts between them reflect seasonal variability in water column structure. Overall, Mg/Ca ratios in *G. ruber* (pink) decrease in association with upwelling and cooler surface waters. By contrast, *O. universa* Mg/Ca is higher during upwelling conditions, consistent with upward migration in the water column (Tedesco et al., 2007; Fig. 5). No difference is seen in *G. menardii*, which reflects lower temperature variability at greater habitat depths.

Sr/Ca Ratio

The Sr/Ca ratios of foraminifera have been associated with a range of environmental conditions. Foraminiferal Sr/Ca has been shown to increase with temperature in some species (Lea et al., 1999; Elderfield et al., 2002; Kisakurek et al., 2008) but not others (Cleroux et al., 2008). The ratio of Sr/Ca has also been shown to increase with salinity (Lea et al., 1999; Kisakurek et al., 2008) and carbonate chemistry variables, such as pH and carbonate saturation state (Lea et al., 1999; Russell et al., 2004; Mortyn et al., 2005; Dissard et al., 2010; Raitzsch et al., 2010; Yu et al., 2014; Keul et al., 2017). None of these proposed drivers are significant predictors of Sr/Ca variability in any of the three species measured here ($p > 0.05$, $r^2 > 0.01$). Additionally, Sr/Ca may be influenced by growth rate (Russell et al., 2004; Kisakurek et al., 2008; Dissard et al., 2010; but not Keul et al., 2017), or the Sr/Ca ratio of seawater (Delaney et al., 1985; Elderfield et al., 2002), though neither could be directly tested here. While Sr/Ca is lower in *G. ruber* (pink), it is higher in *G. menardii* during upwelling conditions, potentially consistent with a greater change in upwelling-associated temperature and pH within the habitat of *G. ruber* compared to *G. menardii*, whose depth habitat may shoal and contract during upwelling events (Figure 5).

Mn/Ca Ratio

The Mn/Ca of planktic foraminifera has been used to trace the influence of diagenesis and contamination, specifically overgrowths of manganese oxides, with non-biogenic, high Mg/Ca ratios (e.g., Boyle, 1983; Pena et al., 2005; van Raden et al., 2011). However, studies in both fossil and living foraminifera have shown that Mn can also be incorporated into original calcite. Culture work in the benthic foraminifera *Ammonia tepida* shows that shell Mn/Ca ratios increase with seawater [Mn] (Munsel et al., 2010) and benthic foraminiferal Mn/Ca has been interpreted as an oxygen indicator, with higher Mn/Ca ratios used to show a decrease in Oxygen Minimum Zone intensity (less complete remineralization in the overlying water column; Klinkhammer et al., 2009) or a shift from an oxic to hypoxic benthos (Groeneveld & Filipsson, 2013; McKay et al., 2015). In sediment records, the Mn/Ca signal in planktic foraminifera has been interpreted as increased terrestrial influx (Klinkhammer et al., 2009), a tracer of surface water masses (Marr et al., 2013), or reflective of water column oxygenation (Steinhardt et al., 2014).

Here, Mn/Ca is interpreted as original to the foraminiferal calcite as specimens recovered using plankton tows will not have undergone alteration in the sediment. It is possible to introduce Mn-rich contaminant phases in the water column or during preservation, and contaminant phases have been observed to occur preferentially on the inner or outer shell (Pena et al., 2005; van Raden et al., 2011; Gibson et al., 2016). However, LA ICP-MS profiles of Mn/Ca do not show this type of contamination. Moreover, SEM images show excellent preservation (Appendix Fig. S1) and an absence of shell surface overgrowths (see figure 4 in Gibson et al., 2016). An environmental control in the water column is therefore implicated as the source of Mn/Ca variability, rather than reflecting sample handling or preservation.

In the Cariaco Basin, there are two possible sources for temporal variability in Mn concentrations: terrestrial inputs or upwelling of Mn-enriched deep waters. Previous work shows that seawater [Mn] is a control on Mn/Ca (Munsel et al., 2010; Barras et al., 2018; van Dijk et al., 2019). We therefore assume that shell Mn/Ca ratios are dependent on the availability of Mn, and in particular [Mn^{2+}] in near-surface waters on sub-annual time scales. We hypothesize that a terrestrial source would most likely be associated with the timing of increased riverine outflows, roughly opposite that of upwelling, and decreased surface salinity. In contrast, a deep water source for elevated Mn, would be associated with an increased influence of upwelled water masses and more elevated values in deeper-dwelling species. A [Mn^{2+}] maximum is present near the oxic/anoxic boundary, at 200–300 m in Cariaco Basin (Jacobs et al., 1987; Percy et al., 2008), and although Mn^{2+} is not stable in oxic waters, it can upwell into shallower waters. In fact, elevated Mn/Ca is observed in all three species during periods of upwelling, with the greatest enrichment found in the deepest living species, *G. menardii*, consistent with an upwelled source for Mn^{2+} associated with low-oxygen waters (Figs. 5, S4).

There is no clear relationship between oxygen concentration in the water column and foraminiferal Mn/Ca. This may be due to a mismatch between the temporal resolution of our CTD data (instantaneous), and the foraminifera record (cumulative). It is also possible that the influx of Mn^{2+} to near-surface waters is imperfectly coupled with oxygenation, with advection of Mn^{2+} into the upper 100 m occurring more rapidly than the rate of Mn oxide formation. Therefore, we suggest that shallow planktic foraminifera in the Cariaco Basin incorporate more Mn^{2+} into their shells during upwelling due to increased upward advection of Mn^{2+}-rich waters from near the oxic/anoxic boundary. No published [Mn] values are available for the oxic surface waters in Cariaco Basin, however using the $D_{Mn/Ca}$ reported for *O. universa* of 0.6 (Allen et al., 2016), our full range of *O universa* Mn/Ca, and assuming a [Ca] of $\sim$10 mmol L^{-1}, we would predict [Mn] in seawater ranging between 5 and 1128 nmol L^{-1}. This is broadly consistent with the range of [Mn] found in suboxic Cariaco Basin waters (Percy et al., 2008). A secondary route that cannot be excluded is the ingestion of Mn-enriched prey, as previously observed in mussels feeding on high-Mn algae during productive upwelling periods (Langlet et al., 2007). This may be especially pertinent for *G. menardii*, which both has the most elevated Mn/Ca ratios and may prefer algal prey (Hemleben & Schiebel, 2017).

The unique nature of the shallow oxic/anoxic interface in Cariaco Basin raises a further question as to whether upwelling-associated Mn/Ca enrichment may be limited to foraminifera from Cariaco Basin. In order to test this, our results are compared with two samples of *N. incompta* from plankton tows on the Central California margin. Similar to the Cariaco Basin, this is a region of strong seasonal wind-driven upwelling, associated with underlying low-oxygen waters, but unlike the Cariaco Basin, it is situated along an open shelf environment rather than in a restricted anoxic basin. Here too, we find elevated shell Mn/Ca ratios during upwelling relative to non-upwelling conditions with 7 μmol/mol in the tow taken during non-upwelling fall conditions, and 30 μmol/mol in the upwelling tow in the spring

(Fig. 5). Thus, shell Mn/Ca ratios in pristine calcite may reflect upwelled deep-water masses in multiple environments, and if differentiated from overgrowths and remineralized phases, may serve as a potential tracer for the intrusion of deep water masses into shallower foraminifera habitats.

Ba/Ca Ratio

Both laboratory culture and core top studies show that planktic foraminifera incorporate Ba into their shells in proportion to its concentration in seawater, irrespective of temperature, salinity, or pH (Lea & Boyle, 1991; Hönisch et al., 2011; Fehrenbacher et al., 2018). As such, foraminiferal Ba/Ca ratios are used as a proxy for seawater [Ba], most commonly to represent changes in salinity or terrestrial inputs (e.g., Weldeab et al., 2007; Bahr et al., 2013; Evans et al., 2015; Vetter et al., 2017). However, Ba/Ca ratios that are too high to reflect the [Ba] of ambient seawater have been noted in several non-spinose species, including *G. menardii*, *G. truncatulinoides*, and *N. dutertrei* (Lea & Boyle, 1991; Bahr et al., 2013; Fehrenbacher et al., 2018). In these species, Ba/Ca ratios have been hypothesized to represent either prey choice (Bahr et al., 2013) or Ba enrichment within marine snow, where these species may live (Fehrenbacher et al., 2018).

Significantly higher Ba/Ca values in *G. ruber* (pink) and *O. universa* occur during upwelling and likely reflect the influence of nutrient-rich deep water (Figs. 5, S4). There is also a significant, though weak, linear relationship between chlorophyll *a* integrated over the upper 100 m and elevated Ba/Ca in both *G. ruber* (pink) and *O. universa*. There is no evidence for a fresh-water influence in any species as indicated by timing or comparison with salinity. Thus, in this dynamic upwelling system, it appears that higher Ba/Ca ratios in the spinose planktic foraminifers *G. ruber* (pink) and *O. universa* are indicative of high-productivity, remineralization of Ba in the upper water column, and the upwelling of high Ba waters from deeper in the water column, rather than terrestrial influences. Falkner et al. (1993) report seawater [Ba] < 90 nmol L^{-1} throughout the Cariaco Trench. Given the empirical distribution coefficient for Ba/Ca in spinose foraminifera (Hönisch et al., 2011), this should result in foraminiferal Ba/Ca < 1.4 μmol/mol, assuming [Ca] of $\sim$10 mmol L^{1} and that shells record dissolved Ba in ambient seawater. However, measured Ba/Ca in *G. ruber* (pink) and *O. universa* frequently exceeds these values (ranging between 0.5 and 33.3 μmol/mol, with means of 7.1 and 5.4 μmol/mol for *G. ruber* (pink) and *O. universa*, respectively), thus we hypothesize that these foraminifera must be exposed to an additional source of Ba during upwelling conditions, which could include bioconcentration of Ba or barite in prey and/or within dinoflagellate symbionts. In contrast, *G. menardii* Ba/Ca shows no clear relationship between either productivity or upwelling (Fig. 5). Ratios of Ba/Ca are consistently high in *G. menardii* (ranging from 1.1 to 83.5; mean $=$ 14.6 μmol/mol) (Figs. 5, S4), and our results support previous work showing that Ba/Ca in this species is not reflective of ambient seawater (Lea & Boyle, 1991; Bahr et al., 2013).

SHELL SIZE

Shell size is widely hypothesized to relate to TE composition in foraminifera, with the use of constrained size fractions a standard practice for Mg/Ca paleothermometry. In this study, we find overall larger *O. universa* during non-upwelling conditions, and some relationship between size and TE in all species. It must also be noted that the smallest individual foraminifera measured from these samples was 250 μm, potentially an artifact of the relatively large mesh size used for capture (200 μm). As a result, sampling is skewed away from very small or juvenile forms that may also have been present in the water column.

Size is positively correlated with Mg/Ca in both *O. universa* and *G. ruber* (pink), as has been shown for many planktic species including *O. universa* (Elderfield, 2002; Friedrich et al., 2012), although the causality is uncertain (Fig. 6A). One possibility is that increased growth rate promotes both increased Mg/Ca and greater size. Counter to this hypothesis are two observations. The first is that diurnal banding in foraminifera consists of thinner (thus, likely slower growing), high-Mg/Ca 'night' bands with corresponding thicker, low-Mg/Ca 'day' bands (Spero et al., 2015; Fehrenbacher et al., 2017). The second is the presence of a relatively thick low-Mg/Ca crust in several species, capable of forming under the same hydrologic conditions as ontogenetic calcite (Jonkers et al., 2016; Davis et al., 2017) and likely more rapidly. While these observations can only be linked to growth rate on the scale of hours or days, they are inconsistent with a simple causal link between shell growth rate and high-Mg calcite. Therefore, we hypothesize that overall warmer conditions could promote both increased shell Mg/Ca and higher growth rates (Lombard et al., 2009).

Size has been shown to correspond with higher temperatures over global (Schmidt et al., 2004) and latitudinal (Be et al., 1987) spatial scales as well as within individual cultured foraminifera (Caron et al., 1987; Bijma et al., 1992; Burke et al., 2018). However, temperature is just one of several interacting variables that may influence terminal size based on optimal growth conditions with food availability also associated with larger sizes (e.g., Bijma et al., 1992; Schmidt et al., 2004). Conversely, larger sizes can be associated with suboptimal conditions and delayed reproduction (Mojtahid et al., 2015), which would support our observation of a smaller terminal size in *O. universa* during upwelling (more nutrient rich) conditions. Overall, it appears that the relationship between size and Mg/Ca is not universal. For example, *G. ruber* (white) has alternately been associated with a decrease in Mg/Ca with increasing size (Friedrich et al., 2012) or with size not significantly predicting Mg/Ca at all (Gray et al., 2018).

The relationship between *G. menardii* size and TEs is more difficult to interpret. No relationship was found between size and Mg/Ca, but size is negatively correlated with Sr/Ca (Fig. 6B). These findings are consistent with a decrease in Sr/Ca with increasing size observed in other species (Elderfield et al., 2002). The difference in relationships between size and elemental composition in *G. menardii* compared to spinose *O. universa* and *G. ruber* (pink) may point to a more complex ecology involving greater interaction with highly variable microenvironments or less exposure to temperature variability. It is also possible that ontogeny plays a greater role in *G. menardii* as they are larger and thus a wider range of ontogenetic stages may be represented compared to the smaller *G. ruber* (pink) or *O. universa*, for which only the terminal stage was analyzed. In the Cariaco Basin, size does not correlate with either Ba/Ca or Mn/Ca in any species (Fig. 6). Overall, we find that relationships between size and TEs are inconsistent across species, but may potentially represent optimal growth under differing environmental conditions.

CONCLUSIONS

Analyses of TE/Ca in the shells of three species of planktic foraminifera from monthly plankton tows in the Cariaco Basin show inter-individual, inter-specific, and upwelling-related variability in Mg/Ca, Sr/Ca, Ba/Ca, and Mn/Ca ratios. The population mean Mg/Ca for each species, but not individual shells, approximates temperatures in the upper 100 m of the water column year-round. The Mn/Ca of all three species is elevated during periods of upwelling, which we hypothesize is associated with upward advection of high [Mn^{2+}] waters from the oxic/anoxic boundary. The elevated Mn/Ca composition of *N. incompta* specimens obtained during upwelling conditions from the California Margin supports this hypothesis. Similarly, Ba/Ca ratios in the spinose foraminifers *O. universa* and *G. ruber* (pink), though not *G. menardii*, are found to be associated with periods of higher productivity and upwelling. While populations as a whole largely reflect macroenvironmental variables (temperature, upwelling, and productivity), individual shell TE ratios are influenced by size, ontogeny, and other 'vital effects'. Significant variability across individuals is present in all species and elements and should caution against the over interpretation of individual shell TE ratios in the fossil record. Use of individual chamber and individual shell records may therefore be limited, but could be improved by careful consideration of ecology and species-specific associations with all measured TE, including Ba and Mn, where resolvable from contaminant phases. These later two elements may be particularly useful as tracers of upwelling and deeper water masses.

ACKNOWLEDGMENTS

Many thanks to M. Bizimis for help and advice in the laboratory, to E. Tappa for assistance with figures, and to W. Gray and an anonymous reviewer for their constructive comments and helpful suggestions.

REFERENCES

Allen, K. A., Honisch, B., Eggins, S. M., Haynes, L. L., Rosenthal, Y., and Yu, J., 2016, Trace element proxies for surface ocean conditions: A synthesis of culture calibrations with planktic foraminifera: Geochimica et Cosmochimica Acta, v. 193 197–221.

Anand, P., and Elderfield, H., 2005, Variability of Mg/Ca and Sr/Ca between and within the planktonic foraminifers *Globigerina bulloides* and *Globorotalia truncatulinoides*: Geochemistry, Geophysics, Geosystems, v. 6, doi: 10.1029/2004GC000811.

Anand, P., Elderfield, H., and Conte, M. H., 2003, Calibration of Mg/Ca thermometry in planktonic foraminifera from a sediment trap time series: Paleoceanography, v. 18, p. 1050.

Astor, Y., Muller-Karger, F., and Scranton, M. I., 2003, Seasonal and interannual variation in the hydrography of the Cariaco Basin: Implications for basin ventilation: Continental Shelf Research, v. 23, p. 125–144.

Babila, T. L., Rosenthal, Y., and Conte, M. H., 2014, Evaluation of the biogeochemical controls on B/Ca of *Globigerinoides ruber* white from the Oceanic Flux Program, Bermuda: Earth and Planetary Science Letters, v. 404, p. 67–76.

Bahr, A., Schönfeld, J., Hoffmann, J., Voigt, S., Aurahs, R., Kucera, M., Flögel, S., Jentzen, A., and Gerdes, A., 2013, Comparison of Ba/Ca and as freshwater proxies: A multi-species core-top study on planktonic foraminifera from the vicinity of the Orinoco River mouth: Earth and Planetary Science Letters, v. 383, p. 45–57.

Barras, C., Mouret, A., Nardelli, M. P., Metzger, E., Peterson, J., La, C., Filipsson, H. L., and Jorissen, F., 2018, Experimental calibration of manganese incorporation in foraminiferal calcite: Geochimica et Cosmochimica Acta, v. 237, p. 49–64.

Bijma, J., Hemleben, C., Oberhansli, H., and Spindler, M., 1992, The effects of increased water fertility on tropical spinose planktonic foraminifers in laboratory cultures, Journal of Foraminiferal Research, v. 22, p. 242–256.

Black, D. E., Abahazi, M. A., Thunell, R. C., Kaplan, A., Tappa, E. J., and Peterson, L. C., 2007, An 8-century tropical Atlantic SST record from the Cariaco Basin: Baseline variability, twentieth-century warming, and Atlantic hurricane frequency: Paleoceanography, v. 22, doi: 10.1029/2007PA001427.

Bolton, A., 2011, LA-ICP-MS Trace Element Analysis of Planktonic Foraminifera and Application to Marine Isotope Stage 31 in the Southwest Pacific Ocean. Thesis.

Boyle, E. A., 1983, Manganese carbonate overgrowths on foraminifera tests: Geochimica et Cosmochimica Acta, v. 47, p. 1815–1819.

Branson, O., Fehrenbacher, J. S., Vetter, L., Sadekov, A. Y., Eggins, S. M., and Spero, H. J., 2019, LAtools: A data analysis package for the reproducible reduction of LA-ICPMS data, Chemical Geology, v. 504, p. 93–95.

Burke, J. E., Renema, W., Henehan, M. J., Elder, L. E., Davis, C. V., Maas, A. E., Foster, G. L., Schiebel, R., and Hull, P. M., 2018, Factors influencing test porosity in planktonic foraminifera, Biogeosciences, v. 15, p. 6607–6619, doi: 10.5194/bg-15-6607-2018.

Caron, D. A., Faber, W. W., and Be, A. W. H., 1987, Growth of the spinose planktonic foraminifer *Orbulina universa* in laboratory culture and the effect of temperature on life processes: Journal of the Marine Biological Association of the United Kingdom, v. 67, p. 343–358.

Cleroux, C., Cortijo, E., Anand, P., Labeyrie, L., Bassinot, F., Caillon, N., and Duplessy, J.-C., 2008, Mg/Ca and Sr/Ca ratios in planktonic foraminifera: Proxies for upper water column temperature reconstruction, v. 23, doi: 10-1029/2007PA001505.

Davis, C. V., Fehrenbacher, J. S., Hill, T. M., Russell, A. D., and Spero, H. J., 2017, Relationships Between Temperature, pH, and Crusting on Mg/Ca Ratios in Laboratory-Grown Neogloboquadrina Foraminifera: Paleoceanography, v. 32, p. 1137–1152.

Dekens, P. S., Lea, D. W., Pak, D. K., and Spero, H. J., 2002, Core top calibration of Mg/Ca in tropical foraminifera: Refining paleotemperature estimation: Geochemistry, Geophysics, Geosystems, v. 3, p. 1–29.

Delaney, M. L., Be, A. W. H., and Boyle, E. A., 1985, Li, Sr, Mg, and Na in foraminiferal calcite shells from laboratory culture, sediment traps, and sediment cores: Geochimica et Cosmochimica Acta, v. 49, p. 1327–1341.

Dissard, D., Nehrke, G., Reichart, G.-J., and Bijma, J., 2010, Impact of seawater pCo2 on calcification and Mg/Ca and Sr/Ca ratios in benthic foraminifera calcite: Results from culturing experiments with *Ammonia tepida*: Biogeosciences, v. 7, p. 81–93, doi: 10.5194/bg-7-81-2010.

Dueñas-Bohórquez, A., da Rocha, R. E., Kuroyanagi, A., de Nooijer, L. J., Bijma, J., and Reichart, G.-J., 2011, Interindividual variability and ontogenetic effects on Mg and Sr incorporation in the planktonic foraminifer *Globigerinoides sacculifer*: Geochimica et Cosmochimica Acta, v. 75, p. 520–532.

Eggins, S. M., Sadekov, A., and De Deckker, P., 2004, Modulation and daily banding of Mg/Ca in *Orbulina universa* tests by symbiont photosynthesis and respiration: A complication for seawater thermometry?: Earth and Planetary Science Letters, v. 225, p. 411–419.

Elderfield, H., and Ganssen, G., 2000, Past temperature and $\delta^{18}O$ of surface ocean waters inferred from foraminiferal Mg/Ca ratios: Nature, v. 405, p. 442–445.

Elderfield, H., Vautravers, M., and Cooper, M., 2002, The relationship between shell size and Mg/Ca, Sr/Ca, δ^{18}O, and δ^{13}C of species of planktonic foraminifera, Geochemistry, Geophysics, Geosystems, v. 3, p. 1–13.

Evans, D., Bhatia, R., Stoll, H., and Müller, W., 2015, LA-ICPMS Ba/Ca analyses of planktic foraminifera from the Bay of Bengal: Implications for late Pleistocene orbital control on monsoon freshwater flux: Geochemistry, Geophysics, Geosystems, v. 16, p. 2598–2618.

Falkner, K. K., Klinkhammer, G. P., Bowers, T. S., Todd, J. F., Lewis, B. L., Landing, W. M., and Edmond, J. M., 1993, The behavior of barium in anoxic marine waters: Geochimica et Cosmocchimica Acta, v. 57, p. 537–554.

Fehrenbacher, J. S., Russell, A. D., Davis, C. V., Gagnon, A. C., Spero, H. J., Cliff, J. B., Zhu, Z., and Martin, P., 2017, Link between light-triggered Mg-banding and chamber foraminifer in the planktic foraminifera *Neogloboquadrina dutertrei*: Nature Communications, v. 8, doi: 10.1038/ncomms15441.

Fehrenbacher, J. S., Russell, A. D., Davis, C. V., Spero, H. J., Chu, E., and Honisch, B., 2018, Ba/Ca ratios in the non-spinose planktic foraminifer *Neogloboquadrina dutertrei*: Evidence for an organic aggregate microhabitat: Geochimica et Cosmochimica Acta, v. 236, p. 361–372, doi: 10.1016/j.gca.2018.03.008.

Ford, H. L., Ravelo, A. C., and Polissar, P. J., 2015, Reduced El Niño–Southern Oscillation during the last glacial maximum: Science, v. 347, p. 255–258.

Friedrich, O., Schiebel, R., Wilson, P. A., Weldeab, S., Beer, C. J., Cooper, M. J., and Fiebig, J., 2012, Influence of test size, water depth, and ecology on Mg/Ca, Sr/Ca, δ^{18}O and δ^{13}C in nine modern species of planktic foraminifers: Earth and Planetary Science Letters, v. 319, p. 133–145.

Gast, R. J., and Caron, D. A., 1996, Molecular phylogeny of symbiotic dinoflagellates from Foraminifera and Radiolaria: Molecular Biology and Evolution, v. 13, p. 1192–1197.

Gastrich, M. D., 1987, Ultrastructure of a new intracellular symbiotic alga found within planktonic foraminifera: Journal of Phycology, v. 36, p. 172–177.

Gibson, K. A., Thunell, R. C., Machain-Castillo, M. L., Fehrenbacher, J., Spero, H. J., Wejnert, K., Nava-Fernández, X., and Tappa, E. J., 2016, Evaluating controls on planktonic foraminiferal geochemistry in the Eastern Tropical North Pacific: Earth and Planetary Science Letters, v. 452, p. 90–103.

Goni, M. A., Aceves, H. L., Thunell, R. C., Tappa, E., Black, D., Astor, Y., Varela, R., and Muller-Karger, F., 2003, Biogenic fluxes in the Cariaco Basin: A combined study of sinking particulates and underlying sediments: Deep Sea Research Part I: Oceanographic Research Papers, v. 50, p. 781–807.

Gray, W. R., and Evans, D., 2019, Nonthermal influences on Mg/Ca in planktonic foraminifera: A review of culture studies and application to the last glacial maximum. Paleoceanography and Paleoclimatology, 34, 306–315. https://doi.org/10.1029/2018PA003517.

Gray, W. R., Weldeab, S., Lea, D. W., Rosenthal, Y., Gruber, N., Donner, B., and Fischer, G., 2018, The effects of temperature, salinity, and the carbonate system on Mg/Ca in *Globigerinoides ruber* (white): A global sediment trap calibration: Earth and Planetary Science Letters, v. 482, p. 607–620, doi: 10.1016/j.epsl.2017.11.026.

Groeneveld, J., and Filipsson, H. L., 2013, Mg/Ca and Mn/Ca ratios in benthic foraminifera: The potential to reconstruct past variations in temperature and hypoxia in shelf regions: Biogeosciences, v. 10, p. 5125–5138.

Haarmann, T., Hathorne, E. C., Mohtadi, M., Groeneveld, J., Kölling, M., and Bickert, T., 2011, Mg/Ca ratios of single planktonic foraminifer shells and the potential to reconstruct the thermal seasonality of the water column: Paleoceanography, v. 26, doi: 10.1029/2010PA002091.

Haug, G. H., Hughen, K. A., Sigman, D. M., Peterson, L. C., and Röhl, U., 2001, Southward migration of the Intertropical Convergence Zone through the Holocene: Sciences, v. 293, p. 1304–1308.

Hemleben, C., Spindler, M., and Anderson O. Roger, 1989. Modern Planktonic Foraminifera Springer-Verlag, New York, 363 p. doi: 10.1007/978-1-4612-3544-6.

Henehan, M. J., Foster, G. L., Rae, J. W. B., Prentice, K. C., Erez, J., Bostock, H. C., Marshall, B. J., and Wilson, P. A., 2015, Evaluating the utility of B/Ca ratios in planktic foraminifera as a proxy for the carbonate system: A case study of *Globigerinoides ruber*: Geochemistry, Geophysics, Geosystems, v. 16, p. 1052–1069.

Hönisch, B., Allen, K. A., Russell, A. D., Eggins, S. M., Bijma, J., Spero, H. J., Lea, D. W., and Yu, J., 2011, Planktic foraminifers as recorders of seawater Ba/Ca: Marine Micropaleontology, v. 79, p. 52–57.

Jacobs, L., Emerson, S., and Huested, S. S., 1987, Trace metal geochemistry in the Cariaco Trench: Deep Sea Research Part 1, v. 34, p. 965–981.

Jentzen, A., Schoönfeld, J., and Schiebel, R., 2018a, Assessment of the effect of increasing temperature on the ecology and assemblage structure of modern planktic foraminifers in the Caribbean and surrounding seas: Journal of Foraminiferal Research, v. 48, p. 251–272.

Jentzen, A., Nuürnberg, D., Hathorne, E. C., and Schoönfeld, J., 2018b, Mg/Ca and δ^{18}O in living planktic foraminifers from the Caribbean, Gulf of Mexico and Florida Straits: Biogeosciences, v. 15, p. 7077–7095.

Jochum, K. P., Weis, U., Stoll, B., Kuzmin, D., Yang, Q., Raczek, I., Jacob, D. E., Stracke, A., Birbaum, K., Frick, D. A., Guünther, D., and Enzweiler, J., 2011, Determination of reference values for NIST SRM 610–617 glasses following ISO Guidelines: Geostandards and Geoanalytical Research, v. 35, p. 397–429.

Jochum, K. P., Jentzen, A., Schiebel, R., Stoll, B., Weis, U., Leitner, J., Repschläger, J., Nürnberg, D., and Haug, G. H., 2019, High-resolution Mg/Ca measurements of foraminifer shells using femtosecond LA-ICP-MS for paleoclimate proxy development: Geochemistry, Geophysics, Geosystems, v. 20, p. 2053–2063.

Jones, J. I., 1968, The relationship of planktonic foraminiferal populations to water masses in the western Caribbean and lower Gulf of Mexico: Bulletin of Marine Science, v. 18, p 946–982.

Jonkers, L., Buse, B., Brummer, G.-J., and Hall, I., 2016, Chamber formation leads to Mg/Ca banding in the planktonic foraminifer *Neogloboquadrina pachyderma*: Earth and Planetary Science Letters, v. 451, p. 177–184.

Katz, M. E., Cramer, B. S., Franzese, A., Hönisch, B., Miller, K. G., Rosenthal, Y., and Wright, J. D., 2010, Traditional and emerging geochemical proxies in foraminifera: The Journal of Foraminiferal Research, v. 40, p. 165–192.

Keul, N., Langer, G., Thoms, S., de Nooijer, L., Reichart, G.-J., and Bijma, J., 2017, Exploring foraminiferal Sr/Ca as a new carbonate system proxy: Geochimica et Cosmochimica Acta, v. 202, p. 375–386, doi: 10.1016/j.gca.2016.11.022.

Kisakurek, B., Eisenhauer, A., Bohm, F., Garbe-Schonberg, D., and Erez, J., 2008, Controls on shell Mg/Ca and Sr/Ca in cultured planktonic foraminiferan, *Globigerinoides ruber* (white): Earth and Planetary Science Letters, v. 273, p. 260–269.

Klinkhammer, G. P., Mix, A. C., and Haley, B. A., 2009, Increased dissolved terrestrial input to the coastal ocean during the last deglaciation: Geochemistry, Geophysics, Geosystems, v. 10, doi: 10.1029/2008GC002219.

Langlet, D., Alleman, L., Plisnier, P.-D., Hughes, H., and André, L., 2007, Manganese content records seasonal upwelling in Lake Tanganyika mussels: Biogeosciences, v. 4, p. 195–203.

Lea, D. W., and Boyle, E. A., 1991, Barium in planktonic foraminifera: Geochimica et Cosmochimica Acta, v. 55, p. 3321–3331.

Lea, D. W., Mashiotta, T. A., and Spero, H. J., 1999, Controls on magnesium and strontium uptake in planktonic foraminifera determined by live culturing: Geochimica et Cosmochimica Acta, v. 63, p. 2369–2379.

Lin, H. L., Peterson, L. C., Overpeck, J. T., Trumbore, S. E., and Murray, D. W., 1997, Late Quaternary climate change from δ^{18}O records of multiple species of planktonic foraminifera: High-resolution records from the Anoxic Cariaco Basin, Venezuela: Paleoceanography, v. 12, p. 415–427.

Lombard, F., Erez, J., Michel, E., and Labeyrie, L., 2009, Temperature effect on respiration and photosynthesis of the symbionts-bearing planktonic foraminifera *Globigerinoides ruber, Orbulina universa*, and *Globigerinella siphonifera*: Limnology and Oceanography, v. 54, p. 210–218.

Lorenzoni, L., 2005, The influence of local rivers on the eastern Cariaco Basin, Venezuela. Thesis.

Lorenzoni, L., Thunell, R. C., Benitez-Nelson, C. R., Hollander, D., Martinez, N., Tappa, E., Varela, R., Astor, Y., and Muller-Karger,

F. E., 2009, The importance of subsurface nepheloid layers in transport and delivery of sediments to the eastern Cariaco Basin, Venezuela: Deep Sea Research Part I: Oceanographic Research Papers, v. 56, p. 2249–2262.

Marr, J. P., Baker, J. A., Carter, L., Allan, A. S. R., Dunbar, G. B., and Bostock, H. C., 2011, Ecological and temperature controls on Mg/Ca ratios of *Globigerina bulloides* from the southwest Pacific Ocean: Paleoceanography, v. 26, doi: 10.1029/2010PA002059.

Marr, J. P., Carter, L., Bostock, H. C., Bolton, A., and Smith, E., 2013, Southwest Pacific Ocean response to a warming world: Using Mg/Ca, Zn/Ca, and Mn/Ca in foraminifera to track surface ocean water masses during the last deglaciation: Paleoceanography, v. 28, p. 347–362.

Mashiotta, T. A., Lea, D. W., and Spero, H. J., 1999, Glacial–interglacial changes in Subantarctic sea surface temperature and δ^{18}O-water using foraminiferal Mg: Earth and Planetary Science Letters, v. 170, p. 417–432.

McConnell, M. C., and Thunell, R. C., 2005, Calibration of the planktonic foraminiferal Mg/Ca paleothermometer: Sediment trap results from the Guaymas Basin, Gulf of California: Paleoceanography, v. 20, doi: 10.1029/2004PA001077.

McConnell, M. C., Thunell, R. C., Lorenzoni, L., Astor, Y., Wright, J. D., and Fairbanks, R., 2009, Seasonal variability in the salinity and oxygen isotopic composition of seawater from the Cariaco Basin, Venezuela: Implications for paleosalinity reconstructions: Geochemistry, Geophysics, Geosystems, v. 10, doi: 10.1029/2008GC002035.

McKay, C. L., Groeneveld, J., Filipsson, H. L., Gallego-Torres, D., Whitehouse, M. J., Toyofuku, T., and Romero, O. E., 2015, A comparison of benthic foraminiferal Mn/Ca and sedimentary Mn/Al as proxies of relative bottom-water oxygenation in the low-latitude NE Atlantic upwelling system: Biogeosciences, v. 12, p. 5415–5428.

Mojtahid, M., Manceau, R., Schiebel, R., Hennekam, R. and de Lange, D. J., 2015, Thirteen thousand years of southeastern Mediterranean climate variability inferred from an integrative planktic foraminfieral-based approach: Paleoceanography, v. 30, p. 402–422.

Mortyn, P. G., Elderfield, H., Anand, P., and Greaves, M., 2005, An evaluation of controls on planktonic foraminiferal Sr/Ca: Comparison of water column and core-top data from a North Atlantic transect: Geochemistry, Geophysics, Geosystems, v. 6, doi: 10.1029/2005GC001047.

Muller-Karger, F., Varela, R., Thunell, R., Scranton, M., Bohrer, R., Taylor, G., Capelo, J., Astor, Y., Tappa, E., Ho, T.-Y., and Walsh, J. J., 2001, Annual cycle of primary production in the Cariaco Basin: Response to upwelling and implications for vertical export: Journal of Geophysical Research: Oceans, v. 106, p. 4527–4542.

Muller-Karger, F., Astor, Y., Benitez-Nelson, C. R., Buck, K. N., Fanning, K. A., Lorenzoni, L., Montes, E., Rueda-Roa, D. T., Scranton, M. I., Tappa, E., Taylor, G. T., Thunell, R. C., Troccoli, L., and Varela, R., 2019, The scientific legacy of the CARIACO ocean time-series program: Annual Review of Marine Science, v. 11, p. 413–437.

Munsel, D., Kramar, U., Dissard, D., Nehrke, G., Berner, Z., Bijma, J., Reichart, G. J., and Neumann, T., 2010, Heavy metal incorporation in foraminiferal calcite: Results from multi-element enrichment culture experiments with *Ammonia tepida*: Biogeosciences, v. 7, p. 2339–2350.

Pena, L. D., Calvo, E., Cacho, I., Eggins, S., and Pelejero, C., 2005, Identification and removal of Mn-Mg-rich contaminant phases on foraminiferal tests: Implications for Mg/Ca past temperature reconstructions: Geochemistry, Geophysics, Geosystems, v. 6, doi: 10.1029/2005GC000930.

Percy, D., Li, X., Taylor, G. T., Astor, Y., and Scranton, M. I., 2008, Controls on iron, manganese and intermediate oxidation state sulfur compounds in the Cariaco Basin: Marine Chemistry, v. 111, p. 47–62.

Peterson, L. C., Overpeck, J. T., Kipp, N. G., and Imbrie, J., 1991, A high-resolution Late Quaternary upwelling record from the anoxic Cariaco Basin, Venezuela: Paleoceanography, v. 6, p. 99–119.

Raitzsch, M., Duenas-Bohorquez, A., Reichart, G.-J., de Nooijer, L. J., and Bickert, T., 2010, Incorporation of Mg and Sr in calcite of cultured benthic foraminifera: Impact of calcium concentration and associated calcite saturation state: Biogeosciences, v. 7, p. 869–881, doi: 10.5194/bg-7-869-2010.

Regenberg, M., Steph, S., Nürnberg, D., Tiedemann, R., and Garbe-Schönberg, D., 2009, Calibrating Mg/Ca ratios of multiple planktonic foraminiferal species with δ^{18}O-calcification temperatures: Paleothermometry for the upper water column: Earth and Planetary Science Letters, v. 278, p. 324–336.

Russell, A. D., Hönisch, B., Spero, H. J., and Lea, D. W., 2004, Effects of seawater carbonate ion concentration and temperature on shell U, Mg, and Sr in cultured planktonic foraminifera: Geochimica et Cosmochimica Acta, v. 68, p. 4347–4361.

Sadekov, A., Eggins, S. M., De Deckker, P., and Kroon, D., 2008, Uncertainties in seawater thermometry deriving from intratest and intertest Mg/Ca variability in *Globigerinoides ruber*: Paleoceanography, v. 23, doi: 10.0129/2007PA001452.

Sadekov, A., Eggins, S. M., De Deckker, P., Ninnemann, U., Kuhnt, W., and Bassinot, F., 2009, Surface and subsurface seawater temperature reconstruction using Mg/Ca microanalysis of planktonic foraminifera *Globigerinoides ruber, Globigerinoides sacculifer*, and *Pulleniatina obliquiloculata*: Paleoceanography, v. 24, doi: 10.1029/2008PA001664.

Salmon, K. H., Anand, P., Sexton, P. F., and Conte, M., 2016, Calcification and growth processes in planktonic foraminifera complicate the use of B/Ca and U/Ca as carbonate chemistry proxies: Earth and Planetary Science Letters, v. 449, p. 372–381.

Schiebel, R., and Hemleben, C., 2017, Planktic Foraminifers in the Modern Ocean, Springer-Verlag, Berlin.

Schiebel, R., Smart, S. M., Jentzen, A., Jonkers, L., Morard, R., Meilland, J., Michel, E., Coxall, H. K., Hull, P. M., Garidel-Thoron, T., Aze, T., Quillevere, F., Ren, H., Sigman, D. M., Vonhof, H. B., Martinez-Garcia, A., Kucera, M., Spero, H., Haug, G. H., 2018, Advances in planktonic foraminifer research: New perspectives for paleoceanography: Earth and Planetary Sciences, v. 61, p. 113–138.

Schmidt, D. N., Renaud, S., Bollmann, J., Schiebel, R., and Thierstein, H. R., 2004, Size distribution of Holocene planktic foraminifer assemblages: Biogeography, ecology and adaptation: Marine Micropaleontology, v. 50, p. 319–338.

Scranton, M. I., McIntyre, M., Astor, Y., Taylor, G. T., Müller-Karger, F., and Fanning, K., 2006, Temporal variability in the nutrient chemistry of the Cariaco Basin, *in* Neretin, L. N. (ed.), Past and Present Water Column Anoxia: Springer, Dordrecht, The Netherlands, p. 139–160.

Scranton, M. I., Taylor, G. T., Thunell, R., Benitez-Nelson, C. R., Muller-Karger, F., Fanning, K., Lorenzoni, L., Montes, E., Varela, R., and Astor, Y., 2014, Interannual and subdecadal variability in the nutrient geochemistry of the Cariaco Basin: Oceanography, v. 27, p. 148–159.

Shaked, Y., and de Vargas, C., 2006, Pelagic photosymbiosis: rDNA assessment of diversity and evolution of dinoflagellate symbionts and planktonic foraminiferal hosts: Marine Ecology Progress Series, v. 325, p. 59–71.

Spero, H. J., Eggins, S. M., Russell, A. D., Vetter, L., Kilburn, M. R., and Hönisch, B., 2015, Timing and mechanism for intratest Mg/Ca variability in a living planktic foraminifer: Earth and Planetary Science Letters, v. 409, p. 32–42.

Steinhardt, J., Cléroux, C., Ullgren, J., de Nooijer, L., Durgadoo, J. V., Brummer, G.-J., and Reichart, G.-J., 2014, Anti-cyclonic eddy imprint on calcite geochemistry of several planktonic foraminiferal species in the Mozambique Channel: Marine Micropaleontology, v. 113, p. 20–33.

Steinhardt, J., de Nooijer, L. L. J., Brummer, G.-J., and Reichart, G.-J., 2015, Profiling planktonic foraminiferal crust formation: Geochemistry, Geophysics, Geosystems, v. 16, p. 2409–2430.

Steph, S., Regenberg, M., Tiedemann, R., Mulitza, S., and Nürnberg, D., 2009, Stable isotopes of planktonic foraminifera from tropical Atlantic/Caribbean core-tops: Implications for reconstructing upper ocean stratification: Marine Micropaleontology, v. 71, p. 1–19.

Tedesco, K., and Thunell, R., 2003a, High resolution tropical climate record for the last 6,000 years: Geophysical Research Letters, v. 30, doi: 10.1029/2003GL017959.

Tedesco, K., Thunell, R., Astor, Y., and Muller-Karger, F., 2007, The oxygen isotope composition of planktonic foraminifera from the

Cariaco Basin, Venezuela: Seasonal and interannual variations: Marine Micropaleontology, v. 62, p. 180–193.

Thunell, R. C., Varela, R., Llano, M., Collister, J., Muller-Karger, F., and Bohrer, R., 2000, Organic carbon fluxes, degradation, and accumulation in an anoxic basin: Sediment trap results from the Cariaco Basin: Limnology and Oceanography, v. 45, p. 300–308.

van Dijk, I., Mouret, A., Cotte, M., Le Houedec, S., Oron, S., Reichart, G.-J., Reyes-Herrera, J., Filipsson, H. L., and Barras, C., 2019, Chemical heterogeneity of Mg, Mn, Na, S, and Sr in benthic foraminiferal calcite: Frontiers in Earth Sciences, v. 7, doi: 10.3389/feart.2019.00281.

van Raden, U. J., Groeneveld, J., Raitzsch, M., and Kucera, M., 2011, Mg/Ca in the planktonic foraminifera Globorotalia inflata and *Globigerinoides bulloides* from Western Mediterranean plankton tow and core top samples: Marine Micropaleontology, v. 78, p. 101–112.

Vetter, L., Spero, H. J., Eggins, S. M., Williams, C., and Flower, B. P., 2017, Oxygen isotope geochemistry of Laurentide ice-sheet meltwater across Termination I: Quaternary Science Reviews, v. 178, p. 102–117.

Wejnert, K. E., Thunell, R. C., and Astor, Y., 2013, Comparison of species-specific oxygen isotope paleotemperature equations: Sensitivity analysis using planktonic foraminifera from the Cariaco Basin, Venezuela: Marine Micropaleontology, v. 101, p. 76–88.

Weldeab, S., Lea, D. W., Schneider, R. R., and Andersen, N., 2007, 155,000 years of West African monsoon and ocean thermal evolution: Science, v. 316, p. 1303–1307.

Wit, J., Reichart, G. J., A Jung, S., and Kroon, D., 2010, Approaches to unravel seasonality in sea surface temperatures using paired single-specimen foraminiferal δ^{18}O and Mg/Ca analyses: Paleoceanography, v. 25, doi: 10.1029/2009PA001857.

Yu, J., Elderfield, H., Jin, Z., Tomascak, P., and Rohling, E. J., 2014, Controls on Sr/Ca in benthic foraminifera and implications for seawater Sr/Ca during the late Pleistocene: Quaternary Science Reviews, v. 98, p. 1–6.

Received 6 August 2019
Accepted 29 January 2020

APPENDICES

TABLE S1. Number of individuals of each species analyzed per tow.

FIGURE S1. Scanning Electron Microscope images of uncleaned A) *G. ruber* (pink), B) *O. universa*, and C) *G. menardii* from Cariaco Basin plankton tows to 100 m depth.

FIGURE S2. Crossplots of RSDs for A) Mg/Ca; B) Sr/Ca; C) Ba/Ca; and D) Mn/Ca against the density gradient between the 1 and 100 m. Linear regressions are shown for elements and species where RSD shows a significant relationship to density gradient. We note that the use of linear regression is chosen for visualization purposes and non-linear relationships are possible depending on the underlying environmental driver(s).

FIGURE S3. Temperatures derived from average Mg/Ca of populations represented by at least 10 foraminifera for A) *G. ruber* (pink); B) *O. universa*; and C) *G. menardii*. Multiple published calibrations, both species-specific and multi-species were tested for each, with the source of each relationship shown to the right of the temperature derived. Relationships selected for each species and applied hereafter are shown in bold black lines.

FIGURE S4. Plots of individual A) Mg/Ca; B) Sr/Ca; C) Mn/Ca; D) Ba/Ca; and E) size for *G. ruber* (pink square), *O. universa* (orange triangle), and *G. menardii* (purple circle). The standard deviation of each element after repeat measurements of the final chamber of an individual *G. menardii* is shown in red in the upper left corner of each plot. Periods designated as upwelling are shown as shaded regions. Points have been jittered to increase visibility.

FIGURE S5. Interpolated time series of A) pH and B) salinity from monthly CTD casts (blue dashes). Black boxes from 0 to 100 m show the depth in the water column from which foraminifera were sampled.

These appendices can be found on the Cushman Foundation website in the JFR Article Data Repository (http://www.cushmanfoundation.org/jfr/index.html) as item number JFR_DR2020008